

We are IntechOpen, the world's leading publisher of Open Access books Built by scientists, for scientists

4,800

Open access books available

122,000

International authors and editors

135M

Downloads

Our authors are among the

154

Countries delivered to

TOP 1%

most cited scientists

12.2%

Contributors from top 500 universities



WEB OF SCIENCE™

Selection of our books indexed in the Book Citation Index
in Web of Science™ Core Collection (BKCI)

Interested in publishing with us?
Contact book.department@intechopen.com

Numbers displayed above are based on latest data collected.
For more information visit www.intechopen.com



Atmospheric Radiative Transfer Parameterizations

Feng Zhang, Yi-Ning Shi, Kun Wu, Jiangnan Li and Wenwen Li

Additional information is available at the end of the chapter

<http://dx.doi.org/10.5772/intechopen.82122>

Abstract

Various radiative transfer (RT) schemes are presented in the chapter including four-stream discrete ordinates adding method (4DDA), four-stream harmonic expansion approximation (4SDA) for the solar spectra and absorption approximation (AA), variational iteration method (VIM) for the infrared spectra. 4DDA uses Gaussian quadrature method to deal with the integration in the RT equation. 4SDA considers four-order spherical harmonic expansion in radiative intensity. VIM allows the zeroth-order solution to be identified as AA, and the scattering effect is included in the first-order iteration. By applying 4DDA/4SDA to a realistic atmospheric profile with gaseous transmission considered, it is found that the accuracy of 4DDA/4SDA is superior to two stream spherical harmonic (Eddington approximation) adding method (2SDA) and two-stream discrete ordinates adding method (2DDA), especially for the cloudy conditions. It is shown that the relative errors of 4DDA/4SDA are generally less than 1% in heating rate, while the relative errors of both 2SDA and 2DDA are over 6%. By applying VIM to a full radiation algorithm a gaseous transmission, it is found that VIM is generally more accurate than the discrete ordinates method (DOM). Computationally, VIM is slightly faster than DOM in the two-stream case but more than twice as fast in the four-stream case. In view of its high overall accuracy and computational efficiency, 4DDA, 4SDA, as well as VIM are well suited in solving radiative transfer in climate models.

Keywords: atmospheric radiative transfer, solar four-stream discrete ordinates adding method, solar four-stream harmonic expansion approximation, infrared variational iteration method, infrared absorption approximation, integro-differential equation

1. Introduction

Solving the radiative transfer (RT) equation is a key issue when dealing with solar/infrared radiative processes related to climate simulations (e.g., radiative flux and heating rate

calculation at each level of a climate model). In recent decades, numerous approximation techniques have been proposed to solve the RT equation [1–5].

For solar radiation, analytical solutions of various two-stream approximations [6] have been widely used in climate models [7]. More accurate methods of four-stream approximation and six-stream approximation have also been proposed (e.g., [8–13]). Based on the invariance principle [14], an adding method of four-stream discrete ordinates method (DOM) (4DDA) has been proposed. The advantage of the adding method is that it can handle partial cloud in climate models (e.g., [15–17]). 4DDA is much more accurate than the adding method of two-stream DOM (2DDA) in flux and heating rate calculation, especially under cloudy-sky conditions, where cloud plays an important role in radiative transfer with different dynamics and microphysics [18, 19]. Zhang and Li [20] proposed a new solar RT parameterization (4SDA) which is based on four-stream harmonic expansion to simulate RT in climate modeling.

Since scattering is much weaker for infrared radiation than for solar radiation, an absorption approximation (AA) is used in most current climate models [7]. In AA, the scattering phase function is replaced by a δ -function, meaning that scattering is neglected in all but the forward direction. The advantage of AA is that the upward and downward transfer processes are completely separated. If scattering is considered, the upward and downward intensities are coupled. Under this condition, Fu [21] derived an inverse matrix method to deal with multiple scattering in the atmosphere by using the two-stream DOM (2DOM) and the four-stream DOM (4DOM). It is found that 4DOM is more accurate than 2DOM, especially for thin optical depths. Even if scattering is included, TOA errors for 2DOM can still be $>2 \text{ W m}^{-2}$ for cirrus clouds [22]. The 4DOM results tend to be very accurate, but the calculation process is complicated. Zhang et al. [23] apply the four-stream adding method to resolve multilayer infrared RT.

In the past two decades, the variational iteration method (VIM) has been used to deal with many nonlinear problems [24–31]. In addition, VIM has been shown to converge faster to the exact solution than other methods do. An accurate solution can be found for most nonlinear problems in only one or two iterations for small solution domains in VIM [27, 31]. Because of its flexibility, convenience and efficiency, VIM has been applied to various nonlinear equations ([27–29] and many others). In VIM, a nonlinear problem is separated into linear and nonlinear terms, where the latter are usually difficult to deal with and are initially approximated as a first guess. Subsequently, a correction function is constructed by using a general Lagrange multiplier that can be identified optimally via variational theory. Although the infrared RT equation is not a nonlinear equation, it contains an integral term for the scattering, and this is very complicated to deal with. Therefore, VIM is applied to solve the infrared RT equation.

The objective of the chapter is to introduce 4DDA/4SDA scheme [15] for solar RT, AA, and VIM [32] schemes and apply them to resolve solar/infrared radiative transfer in RT models. The simulation results and their comparison to results from the 128-stream discrete ordinates method radiative transfer scheme [33] are shown in Section 4. Finally, a summary is given in Section 5.

2. Parameterizations for solar radiative transfer

The azimuthally averaged solar RT equation is

$$\mu \frac{dI(\tau, \mu)}{d\tau} = I(\tau, \mu) - \frac{\omega}{2} \int_{-1}^1 I(\tau, \mu') P(\mu, \mu') d\mu' - \frac{\omega}{4\pi} F_0 e^{-\tau/\mu_0} P(\mu, -\mu_0) \quad (1)$$

where μ is the cosine of the zenith angle (we use the positive and negative μ to denote the upward and downward light beams, respectively), τ is optical depth, ω is single-scattering albedo, and $P(\mu, \mu')$ is the azimuthally averaged scattering phase function, defining the light incidence at μ' , which is scattered in the direction μ . F_0 is the incoming solar flux and μ_0 is the solar zenith angle. The $P(\mu, \mu')$ can be written as

$$P(\mu, \mu') = \sum_{l=0}^N \omega_l P_l(\mu) P_l(\mu') \quad (2)$$

where P_l is the Legendre function. The ω_l can be determined from the orthogonal property of Legendre polynomials: $\omega_l = [(2l + 1)/2] \int P(\cos \Theta) P_l(\cos \Theta) d \cos \Theta$. In our notations, $\omega_0 = 1$ and $\omega_1 = 3g$. g is the asymmetry factor.

2.1. Four-stream discrete ordinates scheme

The four-stream discrete ordinates scheme (4DDA) use the Gaussian quadrature method to deal with the integration in Eq. (1). Eq. (1) yields

$$\mu_i \frac{dI(\tau, \mu_i)}{d\tau} = I(\tau, \mu_i) - \frac{\omega}{2} \sum_{l=0}^3 \omega_l P_l(\mu_i) \sum_{j=-2}^2 I(\tau, \mu_j) P_l(\mu_j) a_j - \frac{\omega}{4\pi} F_0 e^{-\tau/\mu_0} \sum_{l=0}^3 \omega_l P_l(\mu_i) P_l(-\mu_0) \quad (3)$$

where the quadrature point $\mu_{-i} = -\mu_i$, the weight $a_{-i} = a_i$ with $i = \pm 1, \pm 2$, $\mu_1 = 0.2113248$, $\mu_2 = 0.7886752$ and $a_1 = a_2 = 0.5$.

After a lengthy and laborious derivation, the solution of (3) is given by

$$\begin{bmatrix} I(\tau, \mu_2) \\ I(\tau, \mu_1) \\ I(\tau, \mu_{-1}) \\ I(\tau, \mu_{-2}) \end{bmatrix} = \begin{bmatrix} \varphi_2^+ e_2 & \varphi_1^+ e_1 & \varphi_1^- e_3 & \varphi_2^- e_4 \\ \varphi_2^+ e_2 & \varphi_1^+ e_1 & \varphi_1^- e_3 & \varphi_2^- e_4 \\ \varphi_2^- e_2 & \varphi_1^- e_1 & \varphi_1^+ e_3 & \varphi_2^+ e_4 \\ \varphi_2^- e_2 & \varphi_1^- e_1 & \varphi_1^+ e_3 & \varphi_2^+ e_4 \end{bmatrix} G + \begin{bmatrix} Z_2^+ \\ Z_1^+ \\ Z_1^- \\ Z_2^- \end{bmatrix} \exp(-\tau/\mu_0) \quad (4)$$

where G is determined by the boundary conditions, and values of other parameters are shown in [13].

The adding method which is used to deal with multilayer RT is shown in [13].

2.2. Four-stream spherical harmonic expansion scheme

The purpose of the four-stream spherical harmonic expansion (4SDA) is to separate out the angle-dependent intensity by assuming

$$I(\tau, \mu) = \sum_{l=0}^3 I_l(\tau) P_l(\mu) \quad (5)$$

By substituting Eqs. (2) and (5) into Eq. (1) and using the orthogonality relation of the Legendre function in $-1 \leq \mu \leq 1$, we obtain

$$\frac{dI_1}{d\tau} = a_0 I_0 - b_0 e^{-\tau/\mu_0} \quad (6)$$

$$2 \frac{dI_2}{d\tau} + \frac{dI_0}{d\tau} = a_1 I_1 - b_1 e^{-\tau/\mu_0} \quad (7)$$

$$3 \frac{dI_3}{d\tau} + 2 \frac{dI_1}{d\tau} = a_2 I_2 - b_2 e^{-\tau/\mu_0} \quad (8)$$

$$3 \frac{dI_2}{d\tau} = a_3 I_3 - b_3 e^{-\tau/\mu_0} \quad (9)$$

The solution of Eqs. (6)–(9) is

$$\begin{bmatrix} I_0 \\ I_1 \\ I_2 \\ I_3 \end{bmatrix} = \begin{bmatrix} e_1 & e_3 & e_2 & e_4 \\ R_1 e_1 & -R_1 e_3 & R_2 e_2 & -R_2 e_4 \\ \hat{P}_1 e_1 & \hat{P}_1 e_3 & \hat{P}_2 e_2 & \hat{P}_2 e_4 \\ Q_1 e_1 & -Q_1 e_3 & Q_2 e_2 & -Q_2 e_4 \end{bmatrix} G + \begin{bmatrix} \eta_0 \\ \eta_1 \\ \eta_2 \\ \eta_3 \end{bmatrix} \exp(-\tau/\mu_0) \quad (10)$$

where G is determined by the boundary conditions, and values of other parameters can be found at [20].

The 4SDA can also be applied to solve multilayer solar RT. The detailed process can be found at [20].

3. Parameterizations for infrared radiative transfer

The infrared RT equation for intensity $I(\tau, \mu)$ is

$$\mu \frac{dI(\tau, \mu)}{d\tau} = I(\tau, \mu) - (1 - \omega) B(\tau) - \frac{\omega}{2} \int_{-1}^1 I(\tau, \mu') P(\mu, \mu') d\mu' \quad (11)$$

where μ , τ , ω , and P are the same as one in Eq. (1). The Planck function is approximated exponentially in optical depth [17, 18] as $B(\tau) = B_0 e^{-\beta\tau}$ where $\beta = -[\ln(B_1/B_0)]/\tau_1$. τ_1 is the optical depth of the considered layer. Planck functions B_0 and B_1 are evaluated by the temperature of the top ($\tau = 0$) and bottom ($\tau = \tau_1$) of the layer, respectively.

3.1. Absorption approximation

In absorption approximation (AA), the scattering phase function $P(\mu, \mu')$ is simplified as a $\delta(\mu, \mu')$ function [22], and the infrared RT equation becomes

$$\mu \frac{dI^0(\tau, \mu)}{d\tau} = (1 - \omega)I^0(\tau, \mu) - (1 - \omega)B_0 e^{-\beta\tau} \quad (12)$$

We use I^0 as the radiative intensity from the absorption approximation. The solution of Eq. (12) is

$$I^0(\tau, \pm\mu) = \left[I^0(\tau_s, \pm\mu) \mp \frac{1 - \omega}{\mu\beta \pm (1 - \omega)} B_0 e^{-\beta\tau_s} \right] e^{\pm(1-\omega)(\tau-\tau_s)/\mu} \pm \frac{1 - \omega}{\mu\beta \pm (1 - \omega)} B_0 e^{-\beta\tau} \quad (13)$$

where $\pm\mu$ is corresponding to the upward (downward) path and τ_s is the initial point at optical depth $\tau_s = 0$ for the downward direction and at $\tau_s = \tau_1$ for the upward direction. Generally, AA is applied to the two-stream case (δ -2AA) and the four-stream case (δ -4AA). In the following subsection, the AA solution is used as the initial approximate solution of the VIM.

3.2. Variational iteration method

A general nonlinear system is used to illustrate the basic idea of variational iteration method (VIM) [24–31]:

$$Lv(x) + Nv(x) = h(x) \quad (14)$$

where $v(x)$ is the function to be solved and $h(x)$, L , and N are an inhomogeneous term, a linear operator, and a nonlinear operator, respectively. If $v(x)$ is found in the (n)th iteration, the ($n + 1$)th-order functional solution is

$$v^{n+1}(x) = v^n(x) + \int_0^x \lambda(\zeta) [Lv^n(\zeta) + N\tilde{v}^n(\zeta) - h(\zeta)] d\zeta \quad (15)$$

Here, $\tilde{v}^n(\zeta)$ is considered as a restricted variation [i.e., $\hat{\delta}\tilde{v}^n(\zeta) = 0$], where $\hat{\delta}$ represents the variation. The term $\lambda(\zeta)$ is a general Lagrange multiplier and should be identified optimally by using variational theory.

Based on VIM, the functional reiteration of the infrared RT equation can be deduced as

$$I^{n+1}(\tau, \pm\mu) = I^n(\tau, \pm\mu) + \int_{\tau_s}^{\tau} \lambda^{\pm}(s) \left[\frac{dI^n(s, \pm\mu)}{ds} \mp \frac{I^n(s, \pm\mu)}{\mu} \pm \frac{\omega}{2\mu} \int_{-1}^1 \tilde{I}^n(s, \mu') P(\pm\mu, \mu') d\mu' \right. \\ \left. \pm (1 - \omega)B_0 e^{-\beta s/\mu} \right] ds \quad (16)$$

According to VIM theory, under the conditions that $\hat{\delta}I^n(s, \pm\mu)\Big|_{s=\tau_s} = 0$, $\hat{\delta} \int_{\tau_s}^{\tau} \frac{(1-\omega)B_0 e^{-\beta s}}{\mu} ds = 0$ and the restricted variation $\hat{\delta}\tilde{I}^n(s, \mu') = 0$, Eq. (16) yields

$$\hat{\delta}I^{n+1}(\tau, \pm\mu) = [1 + \lambda^\pm(s)]\hat{\delta}I^n(s, \pm\mu)\Big|_{s=\tau} + \hat{\delta} \int_{\tau_s}^{\tau} \left[-\frac{d\lambda^\pm(s)}{ds} \mp \frac{\lambda^\pm(s)}{\mu} \right] I^n(s, \pm\mu) ds \quad (17)$$

For the above correction functional to be stationary [i.e., $\hat{\delta}I^{n+1}(\tau, \pm\mu) = 0$], we require the following stationary conditions:

$$-\frac{d\lambda^\pm(s)}{ds} \mp \frac{\lambda^\pm(s)}{\mu} = 0 \text{ and } \lambda^\pm(s)\Big|_{s=\tau} = -1 \quad (18)$$

Therefore the Lagrangian multiplier $\lambda^\pm(s)$ can be identified as

$$\lambda^\pm(s) = -e^{\pm(\tau-s)/\mu} \quad (19)$$

By substituting Eq. (19) into Eq. (16), we obtain

$$I^{n+1}(\tau, \pm\mu) = I^n(\tau, \pm\mu) - \int_{\tau_s}^{\tau} e^{\pm(\tau-s)/\mu} \left[\frac{dI^n(s, \pm\mu)}{ds} \mp \frac{I^n(s, \pm\mu)}{\mu} \pm \frac{\omega}{2\mu} \int_{-1}^1 I^n(s, \mu') P(\pm\mu, \mu') d\mu' \right. \\ \left. \pm (1-\omega)B_0 e^{-\beta s/\mu} \right] ds \quad (20)$$

In two-stream VIM (2VIM), the term of $\int_{-1}^1 I^n(s, \mu') P(\pm\mu, \mu') d\mu'$ in Eq. (22) is simplified as

$$\int_{-1}^1 I^n(s, \mu') P(\pm\mu, \mu') d\mu' = (1 + 3g\mu\mu_1)I^n(s, \mu_1) + (1 + 3g\mu\mu_{-1})I^n(s, \mu_{-1}) \quad (21)$$

where $\mu_1 = -\mu_{-1} = 1/1.66$. The AA expression shown in Eq. (15) is used as the initial zeroth-order solution. By substituting Eq. (15) into Eq. (22), we obtain the first-order solution of upward intensity at $\tau = 0$ and downward intensity at $\tau = \tau_1$. Detailed process can be found at [30]. The upward and downward fluxes are written as

$$F^+(0) = \pi I^1(0, \mu_1) \text{ and } F^-(\tau_1) = \pi I^1(\tau_1, \mu_1) \quad (22)$$

We consider a surface boundary condition with a surface emissivity ε_s as follows in 2VIM

$$I_s(\mu_1) = (1 - \varepsilon_s)I_s(\mu_{-1}) + \varepsilon_s B(T_s) \quad (23)$$

where T_s , $I_s(\mu_1)$, and $I_s(\mu_{-1})$ are the surface temperature, upward intensity, and downward intensity, respectively, at the surface.

In four-stream VIM (4VIM), the term of $\int_{-1}^1 I^n(s, \mu') P(\pm\mu, \mu') d\mu'$ in Eq. (22) is simplified as

$$\int_{-1}^1 I^n(s, \mu') P(\mu_i, \mu') d\mu' = \frac{1}{2} \sum_{j=-2}^2 (1 + 3g\mu_i\mu_j) I^n(s, \mu_j) \quad (24)$$

where $\mu_1 = -\mu_{-1} = 0.2113248$ and $\mu_2 = -\mu_{-2} = 0.7886752$. The AA expression shown in Eq. (15) is used as the initial zeroth-order solution. Detailed process can be found at [30]. The upward and downward fluxes are written as

$$F^+(0) = 2\pi [a_1\mu_1 I^1(0, \mu_1) + a_2\mu_2 I^1(0, \mu_2)] \quad (25)$$

$$F^-(\tau_1) = 2\pi [a_1\mu_1 I^1(\tau_1, \mu_{-1}) + a_2\mu_2 I^1(\tau_1, \mu_{-2})] \quad (26)$$

The surface boundary condition with an emissivity ε_s is given by

$$I_s(\mu_i) = 2(1 - \varepsilon_s) \sum_{j=1}^2 a_j\mu_j I_s(-\mu_j) + \varepsilon_s B(T_s) \quad (27)$$

To enhance the accuracy of the radiative schemes, a δ -function adjustment is used to adjust the optical parameters following Wiscombe [34]. We refer to the VIM solutions with the δ -function applied as δ -2VIM and δ -4VIM.

4. Results and discussion

4.1. Solar spectra

RT in the atmosphere is a complicated process. It depends not only on the single-layer direct reflection and transmission but also on the diffuse results and the gaseous transmission, cloud-aerosol scattering and absorption, etc. It is important to evaluate errors in radiation under a variety of atmospheric conditions by using a radiation algorithm. The Fu-Liou radiation model [35] is used in this study. This model adopts the correlated-k distribution method for gaseous transmission, including five major greenhouse gases, H₂O, CO₂, O₃, NO₂, and CH₄.

In benchmark calculations, the discrete ordinates model [33] with a 128-stream scheme (128S) is incorporated with the gaseous transmission scheme of the Fu-Loiu radiation model [35] by replacing the existing radiative transfer algorithm in the model. Also the two-stream discrete ordinates adding method (2DDA), Eddington adding method (2SDA), four-stream discrete ordinates adding method (4DDA), and four stream spherical harmonic adding method (4SDA) schemes are incorporated with the same gaseous transmission scheme. The atmosphere was vertically divided into 280 layers, each of thickness 0.25 km. The mid-latitude winter of atmospheric profile [36] is used with a surface albedo of 0.2 for each band. For a water cloud the optical properties are parameterized in terms of liquid water content (LWC) and effective

radius (r_e) [36]. Two calculations are performed: (1) a low cloud ($LWC = 0.22\text{gm}^{-3}$, $r_e = 5.89\mu\text{m}$) positioned from 1.0 to 2.0 km and (2) a middle cloud ($LWC = 0.28\text{gm}^{-3}$, $r_e = 6.19\mu\text{m}$) positioned from 4.0 to 5.0 km. Three solar zenith angles of $\mu_0 = 1$, $\mu_0 = 0.5$, and $\mu_0 = 0.25$ are generally considered.

In **Figure 1**, the benchmark results of heating rate are shown for three solar zenith angles under low/middle cloud condition (**Figure 1a–c** for low cloud condition, **Figure 1g–i** for middle cloud condition) as well as the absolute errors of 2DDA, 2SDA, 4DDA, and 4SDA against the benchmark results (**Figure 1d–f** for cloud condition, **Figure 1j–l** for middle cloud condition). When $\mu_0 = 1$, the absolute errors of 2DDA are up to about 1.5 and 2.3 K day^{-1} (relative errors about 6%) for the low and middle clouds. The error of 2SDA is smaller than 2DDA. When $\mu_0 = 0.25$, the result becomes opposite as the error of 2SDA becomes larger than 2DDA. By using 4DDA and 4SDA, relative errors are much suppressed. In general, the relative error becomes less than 1% for the three solar zenith angles. This indicates both 4DDA and 4SDA are accurate enough to obtain cloud-top solar heating.

4.2. Infrared spectra

For the infrared spectra, the accuracy and efficiency of δ -2AA, δ -4AA, δ -2VIM, δ -4VIM, δ -2DOM, and δ -4DOM will be systematically compared. In addition, the discrete ordinates model [28] with a 128-stream scheme (δ -128DOM) is used as the benchmark model.

A radiation model [17] is used to study the accuracy of the VIM scheme for multiple layers within a model atmosphere. A correlation-k distribution scheme is used to simulate the gaseous transmission with profiles for H_2O , CH_4 , CO_2 , NO_2 , O_3 , and CFCs. This model is reasonably efficient because it neglects to scatter for certain intervals with very large absorption coefficients and water vapor continuum at high altitudes. Nine infrared bands are adopted in this model in wavenumber ranges 0–340, 340–540, 540–800, 800–980, 980–1100, 1100–1400, 1400–1900, 1900–2200, and 2200–2500 cm^{-1} . The optical properties of ice and water clouds are calculated based on the radiative property parameterization of [37–39], respectively. The mid-latitude winter atmospheric profiles [36] are used. The atmospheric profile is divided into homogeneous layers with a geometrical thickness of 0.25 km.

In this model, a low cloud with an effective radius $r_e = 5.89\mu\text{m}$ and liquid water content $LWC = 0.22\text{gm}^{-3}$ is located at 1.0–2.0 km, a middle cloud with $r_e = 5.89\mu\text{m}$ and $LWC = 0.22\text{gm}^{-3}$ is located at 4.0–5.0 km, and a high cloud with a mean effective size $D_e = 41.1\mu\text{m}$ and an ice water content $IWC = 0.0048\text{gm}^{-3}$ is located at 9.0–11.0 km. The surface emissivity ϵ_s is set to 1.

In the left column of **Figure 2**, the benchmark heating rates calculated by δ -128DOM are given under conditions of low clouds (**Figure 2a**), middle clouds (**Figure 2d**), high clouds (**Figure 2g**) and the all-sky case containing a combination of low, middle, and high clouds (**Figure 2j**). The middle column of **Figure 2** shows the errors in the calculated heating rates of δ -2AA, δ -2DOM, and δ -2VIM compared to those of δ -128DOM. Furthermore, the right column of **Figure 2** shows the errors in the calculated heating rates of δ -4AA, δ -4DOM, and δ -4VIM compared to those of δ -128DOM.

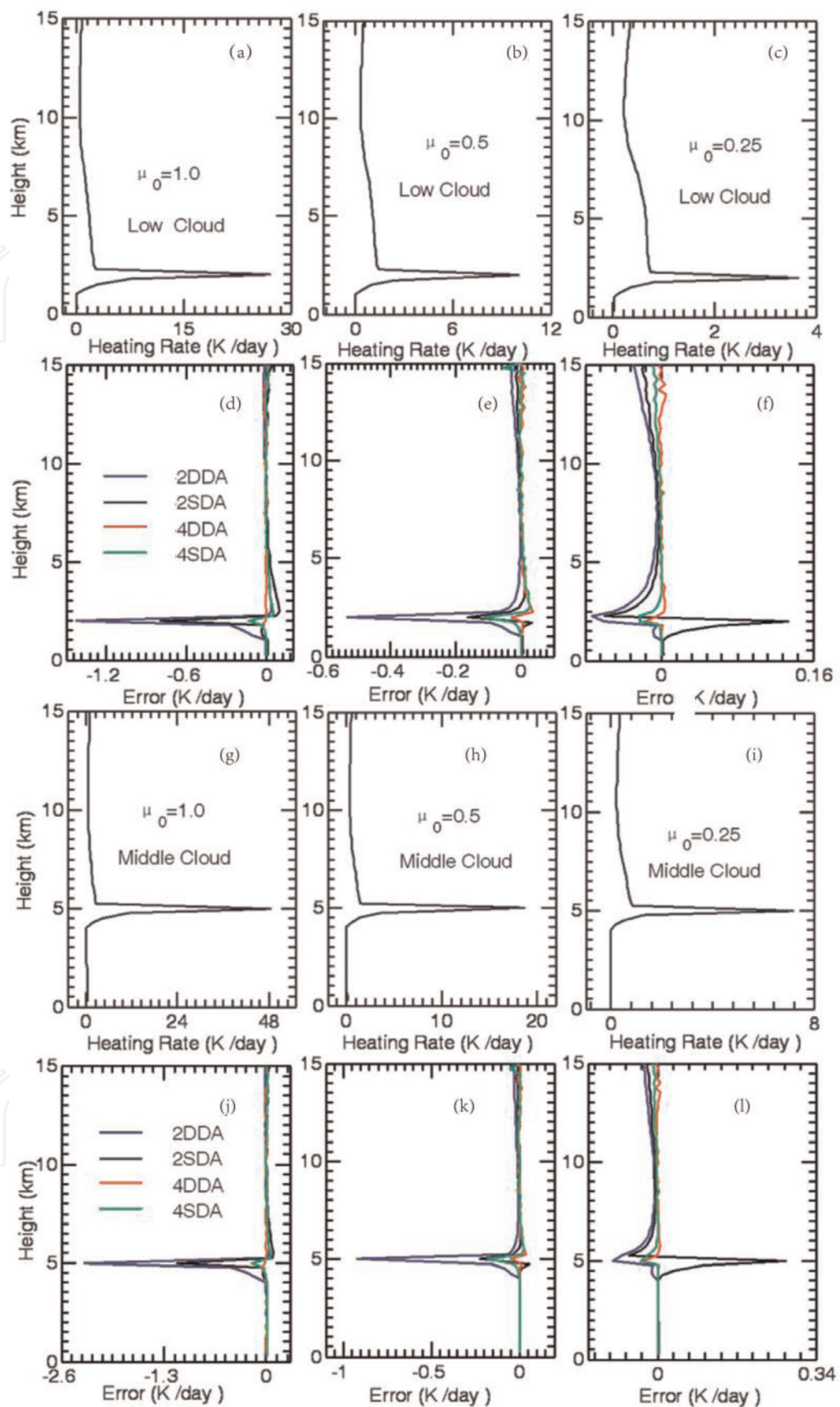


Figure 1. Heating rate profiles computed from 128S and the error profiles from 2DDA, 2SDA, 4DDA, and 4SDA. Three solar zenith angles $\mu_0 = 1$, $\mu_0 = 0.5$, and $\mu_0 = 0.25$ are considered.

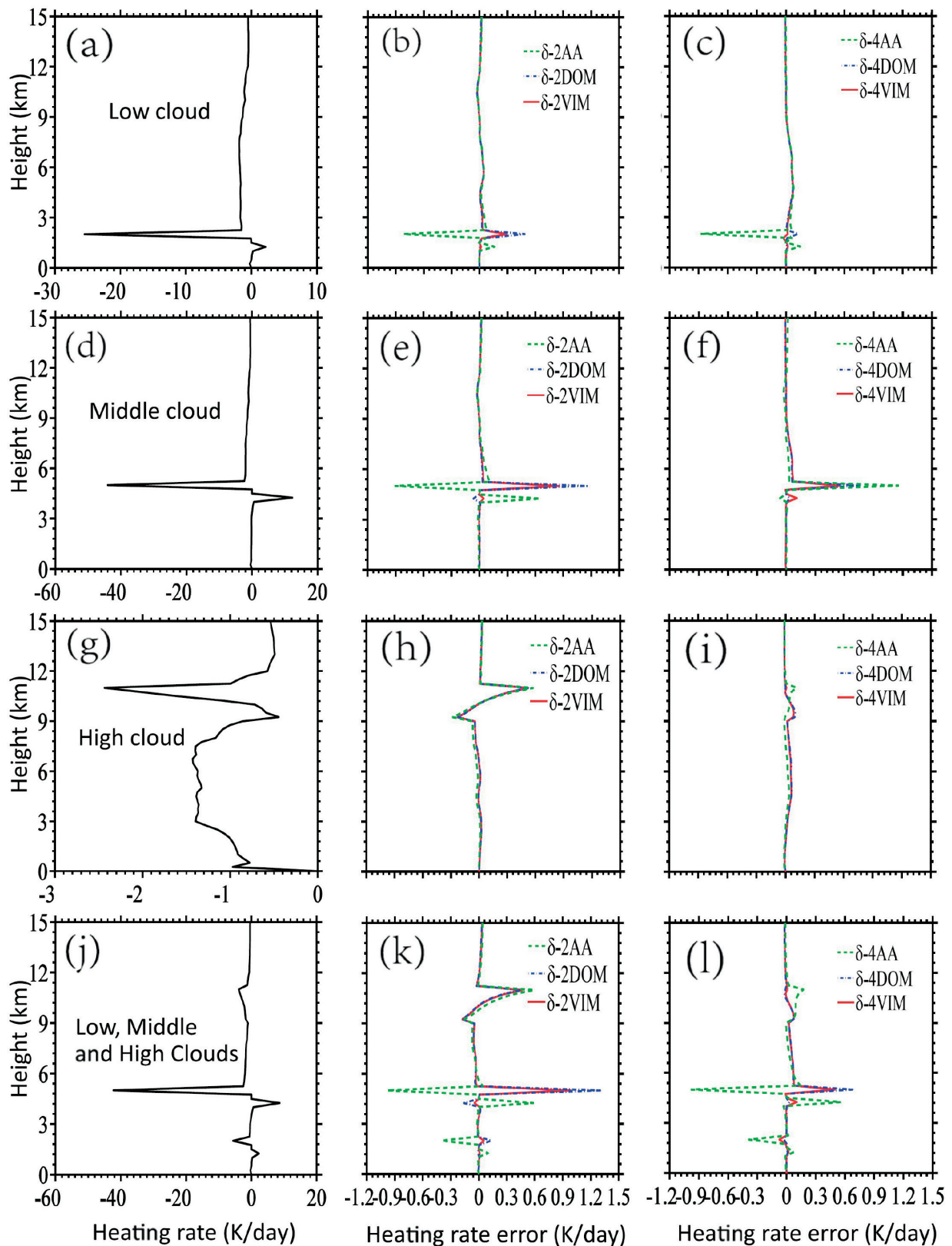


Figure 2. Heating rate profiles calculated by δ -128DOM and the error profiles produced by δ -2AA, δ -4AA, δ -2DOM, δ -4DOM, δ -2VIM, and δ -4VIM in the mid-latitude winter atmospheric profile with surface emissivity $\epsilon_s = 1$ for (a)–(c) low cloud, (d)–(f) middle cloud, (g)–(i) high cloud, and (j)–(l) all three cloud types.

For the low-cloud case, the maximum errors of δ -2AA, δ -2DOM, and δ -2VIM are 20.8, 10.5, and 10.3 K day⁻¹, respectively, at a height corresponding to the top of the cloud (**Figure 2b**). The maximum errors of δ -4AA, δ -4DOM, and δ -4VIM are 20.9, 10.1, and 10.03 K day⁻¹, respectively, at the same height (**Figure 2c**). This shows that, for low-level water clouds, δ -2VIM (δ -4VIM) is more accurate than δ -2AA (δ -4AA) and δ -2DOM (δ -4DOM).

For the middle cloud, the maximum errors of δ -2AA, δ -2DOM, and δ -2VIM are approximately 20.9, 11.1, and 10.8 K day⁻¹, respectively, at a height corresponding to the top of the cloud. At the bottom of the cloud, the errors are 10.6 K day⁻¹ for δ -2AA and just 20.05 and 10.05 K day⁻¹ for δ -2DOM and δ -2VIM, respectively (**Figure 2e**). At the top of the cloud, δ -4AA, δ -4DOM, and δ -4VIM produce biases of approximately 11.1, 10.7, and 10.5 K day⁻¹, respectively (**Figure 2f**).

For the high-cloud case, the optical depth of the ice cloud is much smaller than that of the water cloud. Based on the results shown in **Figure 2**, the accuracies of δ -2DOM and δ -2VIM are similar and are better than that of δ -2AA. Furthermore, δ -4AA, δ -4DOM, and δ -4VIM have very similar accuracies. As seen in the third row in **Figure 2**, δ -2AA produces an error of approximately 10.6 K day⁻¹ at a height corresponding to the top of a high cloud. The

Atmospheric condition	128DOM	2AA	2DOM	2VIM	4AA	4DOM	4VIM
Upward flux (TOA)							
Low clouds	209.5326	211.2735 (1.7409)	208.5206 (-1.012)	209.0425 (-0.4901)	210.9585 (1.4259)	209.1645 (-0.3681)	209.5458 (0.0132)
Middle clouds	183.5646	185.7200 (2.1554)	182.4027 (-1.1619)	182.9060 (-0.6586)	182.4002 (-1.1644)	183.1096 (-0.4550)	183.5357 (-0.0289)
High clouds	198.1357	200.3545 (2.2188)	198.6394 (0.5037)	198.8373 (0.7016)	199.2441 (1.1084)	197.2351 (-0.9006)	197.4354 (-0.7003)
Low, middle, and high clouds	176.3821	179.7768 (3.3947)	175.6421 (-0.7400)	176.2356 (-0.1465)	178.8788 (2.4967)	175.5891 (-0.7930)	175.8856 (-0.4965)
Mean square error		6.0309	0.7939	0.2969	2.7128	0.4456	0.1845
Downward flux (surface)							
Low clouds	302.7236	302.7267 (0.0031)	302.9533 (0.2297)	302.9384 (0.2148)	302.7429 (0.0193)	302.8662 (0.1426)	302.8449 (0.1213)
Middle clouds	287.4458	286.9155 (-0.5303)	287.7658 (0.3200)	287.6141 (0.1683)	287.7658 (0.3200)	287.5678 (0.1220)	287.5418 (0.096)
High clouds	247.8497	248.0313 (0.1816)	248.3309 (0.4812)	248.3303 (0.4806)	248.2968 (0.4471)	248.5608 (0.7111)	248.6452 (0.7955)
Low, middle, and high clouds	302.1410	302.0497 (-0.0913)	302.4413 (0.3003)	302.4227 (0.2817)	302.0189 (-0.1221)	302.3161 (0.1751)	302.3151 (0.1741)
Mean square error		0.0806	0.1192	0.0962	0.0794	0.1429	0.1718

The flux differences between the six approximate schemes and δ -128DOM are listed in parentheses. All δ symbols are neglected in the table.

Table 1. Comparison of δ -2AA, δ -4AA, δ -2DOM, δ -4DOM, δ -2VIM, and δ -4VIM for flux (W m⁻²) at the top and surface by using the mid-latitude winter atmospheric profile with $\epsilon_s = 1$.

	2AA	4AA	2DOM	4DOM	2VIM	4VIM
Algorithm only	1.0	1.4412	2.2223	14.8195	2.0365	5.3615
Radiation model	1.0	1.1095	1.4114	5.8899	1.3759	2.2739

All δ symbols are neglected in the table.

Table 2. Computing times of δ -2AA, δ -4AA, δ -2DOM, δ -4DOM, δ -2DDA, δ -4DDA, δ -2VIM, and δ -4VIM (normalized by the computing time of δ -2AA).

accuracies of δ -2DOM and δ -2VIM are similar; the maximum errors of both are approximately 10.5 K day^{-1} (**Figure 2h**). The maximum errors of δ -4AA, δ -4DOM, and δ -4VIM are all about 10.1 K day^{-1} (**Figure 2i**). However, the difference is that the maximum errors occur at top of the high cloud for δ -4AA but on the bottom for δ -4DOM and δ -4VIM.

In the case of all three clouds together, δ -2VIM is more accurate than δ -2AA and δ -2DOM for the low and middle clouds (**Figure 2k**). In general, δ -4DOM and δ -4VIM are comparable in accuracy for cloud heating rate (**Figure 2l**).

The results of upward (downward) flux at the TOA (surface) for the six schemes are presented in **Table 1** for mid-latitude winter profiles with the surface emissivity $\varepsilon_s = 1$. For the low and middle clouds, the δ -2AA overestimates the upward flux at TOA by 1.8 and 2.1 W m^{-2} , respectively. The errors of the δ -2DOM are up to 21.0 and 21.2 W m^{-2} , while that of the δ -2VIM is limited to 20.7 W m^{-2} . Also, the δ -4VIM is generally more accurate than the δ -4DOM. However, the results for the high clouds are reversed, with the δ -2VIM errors becoming larger than that of δ -2DOM. For the downward flux at the surface, the AA schemes are generally more accurate than the corresponding DOM and VIM schemes except in the middle-cloud case. We also calculate the mean square error of each scheme. For upward flux at TOA, the mean square error of VIM is generally smaller than one of DOM and AA. However, the mean square error of 2VIM and 4VIM is 0.10 W m^{-2} and 0.17 W m^{-2} , respectively, while the mean square error of 2AA is limited to 0.08 W m^{-2} .

For climate modeling, the efficiency of radiative transfer parameterization is also very important. **Table 2** lists the computing times required for δ -2AA, δ -4AA, δ -2DOM, δ -4DOM, δ -2VIM, and δ -4VIM, which were computed by HP EliteDesk 880 G1 TWR with 8 Intel(R) Core(TM) i7-4790 CPUs, 32-bit operating system, and 8GB memory. The results are normalized to that of δ -2AA. The computational efficiency of δ -2VIM is slightly better than that of δ -2DOM, which took more than double the time of δ -2AA. However, δ -4VIM is more than twice as fast as δ -4DOM for the radiation algorithm alone and the radiation model.

5. Summary and conclusions

The objective of the paper is to introduce 4DDA/4SDA [13, 20] for solar RT, AA, and VIM [32] for infrared RT and applied them to radiative transfer models.

4DDA use Gaussian quadrature method to deal with the integration in the RT equation. 4SDA is based on four-stream harmonic expansion in radiative intensity. By applying 4DDA/4SDA to

a realistic atmospheric profile with gaseous transmission considered, it is found that the accuracy of 4DDA/4SDA is superior to Eddington adding method (2SDA) and two-stream discrete ordinates adding method (2DDA), especially for the cloudy conditions. It is shown that the relative errors of 4SDA are generally less than 1% in heating rate, while the relative errors of both 2SDA and 2DDA are over 6%.

VIM differs from other analytical methods for solving nonlinear differential equations in that it requires neither linearization nor small perturbations. The optimal result is constructed through variation by a Lagrange multiplier. It was found that the scattering term in the infrared RT equation could be dealt with as a nonlinear operator in VIM. By taking the AA solution as the zeroth-order solution, the scattering effect was properly included in the first-order iterative solution.

The six schemes of δ -2AA, δ -4AA, δ -2DOM, δ -4DOM, δ -2VIM, and δ -4VIM were compared systematically against the benchmark results provided by δ -128DOM for a multilayer case. For a multilayer atmosphere, VIM gave more accurate results than those of DOM and AA for the low and middle clouds in both the two- and four-stream cases. However, the errors from VIM for high clouds were similar to those from AA.

Computationally, δ -2VIM and δ -2DDA were slightly faster than δ -2DOM, which took more than double time of δ -2AA. However, δ -4VIM/ δ -4DDA was more than twice as fast as δ -4DOM for both the pure radiation algorithm and the radiation model in a layered, cloudy atmosphere. In general, the main benefit of δ -2VIM was an improved accuracy with a computational time similar to that of δ -2DOM. The main benefit of δ -4VIM/ δ -4DDA was improved computational efficiency with accuracy similar to that of δ -4DOM.

In view of their overall high accuracy and computational efficiency, the conclusion is that 4DDA, 4SDA, δ -2VIM, and δ -4VIM are well suited for parameterizing the solar/infrared RT in climate models.

Acknowledgements

The work is supported by the National Key R&D Program of China (2018YFC1507002) and National Natural Science Foundation of China (41675003 and 41675056).

Author details

Feng Zhang^{1*}, Yi-Ning Shi¹, Kun Wu¹, Jiangnan Li² and Wenwen Li¹

*Address all correspondence to: fengzhang@nuist.edu.cn

1 Key Laboratory of Meteorological Disaster, Ministry of Education, Nanjing University of Information Sciences and Technology, Nanjing, China

2 Canadian Centre for Climate Modelling and Analysis, Environment and Climate Change Canada, University of Victoria, Victoria, British Columbia, Canada

References

- [1] Yi-Ning S, Zhang F, Chan KL, Li W, Lin H, Duan M. An improved Eddington approximation method added delta-scaling effect for solar radiative flux calculation in a vertically inhomogeneous medium. *Journal of Quantitative Spectroscopy and Radiative Transfer*. 2019;**226**:40-50
- [2] Feng Z, Wu K, Li J, Zhang H, Hu S. Radiative transfer in the region with solar and infrared spectra overlap. *Journal of Quantitative Spectroscopy and Radiative Transfer*. 2018;**219**:366-378
- [3] Yi-Ning S, Zhang F, Yan J-R, Iwabuchi H, Wang Z. The standard perturbation method for infrared radiative transfer in a vertically internally inhomogeneous scattering medium. *Journal of Quantitative Spectroscopy and Radiative Transfer*. 2018;**213**:149-158
- [4] Feng Z, Yan J-R, Li J, Wu K, Iwabuchi H, Shi Y-N. A new radiative transfer method for solar radiation in a vertically internally inhomogeneous medium. *Journal of the Atmospheric Sciences*. 2018;**75**:41-55
- [5] Wu K, Zhang F, Iwabuchi H, Shi Y-N, Duan M. Double-delta-function adjustment in thermal radiative transfer. *Infrared Physics & Technology*. 2017;**86**:139-146
- [6] Meador WE, Weaver WR. Two-stream approximations to radiative transfer in planetary atmospheres: A unified description of existing methods and a new improvement. *Journal of the Atmospheric Sciences*. 1980;**37**:630-643
- [7] Oreopoulos L et al. The continual intercomparison of radiation codes: Results from phase I. *Journal of Geophysical Research*. 2012;**117**:D06118
- [8] Liou K-N, Fu Q, Ackerman TP. A simple formulation of the delta-four-stream approximation for radiative transfer parameterizations. *Journal of the Atmospheric Sciences*. 1988;**45**:1940-1947
- [9] Li J, Ramaswamy V. Four-stream spherical harmonic expansion approximation for solar radiative transfer. *Journal of the Atmospheric Sciences*. 1996;**53**:1174-1186
- [10] Zhang H, Zhang F, Fu Q, Shen Z, Lu P. Two- and four-stream combination approximations for computation of diffuse actinic fluxes. *Journal of the Atmospheric Sciences*. 2010;**67**:3238-3252
- [11] van Oss RF, Spurr RJ. Fast and accurate 4 and 6 stream linearized discrete ordinate radiative transfer models for ozone profile retrieval. *Journal of Quantitative Spectroscopy & Radiative Transfer*. 2002;**75**:177-220
- [12] Lin L, Fu Q, Zhang H, Su J, Yang Q, Sun Z. Upward mass fluxes in tropical upper troposphere and lower strato-sphere derived from radiative transfer calculations. *Journal of Quantitative Spectroscopy & Radiative Transfer*. 2013;**117**:114-122

- [13] Zhang F, Shen Z, Li J, Zhou X, Ma L. Analytical delta-four-stream doubling-adding method for radiative transfer parameterizations. *Journal of the Atmospheric Sciences*. 2013;**70**:794-808
- [14] Chandrasekhar S. *Radiative Transfer*. London (Oxford University Press)
- [15] Chou M-D, Suarez MJ. A solar radiation parameterization for atmospheric studies. NASA Technical Memorandum: NASA/TM-1999-104606. Vol. 15; 1999. 40pp
- [16] Nakajima T, Tsukamoto M, Tsushima Y, Numaguti A, Kimura T. Modeling of the radiative process in an atmospheric general circulation model. *Applied Optics*. 2000;**39**:4869-4878
- [17] Li J, Barker HW. A radiation algorithm with correlated-k distribution. Part I: Local thermal equilibrium. *Journal of the Atmospheric Sciences*. 2005;**62**:286-309
- [18] Lu C, Liu Y, Niu S, Endo S. Scale dependence of entrainment-mixing mechanisms in cumulus clouds. *Journal of Geophysical Research – Atmospheres*. 2014;**119**:13877-13890
- [19] Lu C, Liu Y, Zhang GJ, Wu X, Endo S, Cao L, et al. Improving parameterization of entrainment rate for shallow convection with aircraft measurements and large-eddy simulation. *Journal of the Atmospheric Sciences*. 2016;**73**:761-773
- [20] Zhang F, Li J. Doubling-adding method for delta-four-stream spherical harmonic expansion approximation in radiative transfer parameterization. *Journal of the Atmospheric Sciences*. 2013;**70**:3084-3101
- [21] Fu Q. Parameterization of radiative processes in vertically nonhomogeneous multiple scattering atmospheres [PhD thesis]. University of Utah; 1991. 259pp
- [22] Li J, Fu Q. Absorption approximation with scattering effect for infrared radiation. *Journal of the Atmospheric Sciences*. 2000;**57**:2905-2914
- [23] Zhang F, Wu K, Li J, Zhao J-Q, Li J. Analytical infrared delta-four-stream adding method from invariance principle. *Journal of the Atmospheric Sciences*. 2016;**73**:4171-4188
- [24] He JH. Variational iteration method for delay differential equations. *Communications in Nonlinear Science and Numerical Simulation*. 1997;**2**:235-236
- [25] He JH. Variational iteration method—A kind of non-linear analytical technique: Some examples. *International Journal of Non-Linear Mechanics*. 1999;**34**:699-708
- [26] He JH. Variational iteration method—Some recent results and new interpretations. *Journal of Computational and Applied Mathematics*. 2007;**207**:3-7
- [27] Tatari M, Dehghan M. On the convergence of He's variational iteration method. *Journal of Computational and Applied Mathematics*. 2007;**207**:121-128
- [28] Liu H, Xiao A, Su L. Convergence of variational iteration method for second-order delay differential equations. *Journal of Applied Mathematics*. 2013;**2013**:634670

- [29] Jafari H. A comparison between the variational iteration method and the successive approximations method. *Applied Mathematics Letters*. 2014;**32**:1-5
- [30] Al-Sawoor AJ, Al-Amr MO. Numerical solution of a reaction-diffusion system with fast reversible reaction by using Adomian's decomposition method and He's variational iteration method. *AL-Rafidain Journal of Computer Sciences and Mathematics*. 2012;**9**(2): 243-257
- [31] Al-Sawoor AJ, Al-Amr MO. A new modification of variational iteration method for solving reaction-diffusion system with fast reversible reaction. *Journal of the Egyptian Mathematical Society*. 2014;**22**:396-401
- [32] Zhang F, Yi-Ning S, Li J, Iwabuchi H. Variational iteration method for infrared radiative transfer in a scattering medium. *Journal of the Atmospheric Sciences*. 2017;**74**:419-430
- [33] Stamnes K, Tsay SC, Wiscombe WJ, Jayaweera K. Numerically stable algorithm for discrete ordinate method radiative transfer in multiple scattering and emitting layered media. *Applied Optics*. 1988;**27**:2502-2509
- [34] Wiscombe W. The delta-M method: Rapid yet accurate radiative flux calculations. *Journal of the Atmospheric Sciences*. 1977;**34**:1408-1422
- [35] Qiang F, Liou KN. On the correlated k-distribution method for radiative transfer in nonhomogeneous atmospheres. *Journal of the Atmospheric Sciences*. 1992;**49**:2139-2156
- [36] McClatchey RA, Fenn RW, Selby JEA, Volz FE, Garing JS. Optical properties of the atmosphere. Air Force Report: AFCRL-71-0279; 1972. 85pp
- [37] Fu Q. Parameterization of radiative processes in vertically nonhomogeneous multiple scattering atmospheres [PhD dissertation]. University of Utah, 1991; 259pp [Available from: University Microfilm, 305 N. Zeeb Rd., Ann Arbor, MI 48106]
- [38] Yang P, Liou K, Bi L, Liu C, Yi B, Baum B. On the radiative properties of ice clouds: Light scattering, remote sensing, and radiation parameterization. *Advances in Atmospheric Sciences*. 2015;**32**:32-63
- [39] Lindner TH, Li J. Parameterization of the optical properties for water clouds in the infrared. *Journal of Climate*. 2000;**13**:1797-1805